Journal of Electrostatics 92 (2018) 38–44

Contents lists available at ScienceDirect

Journal of Electrostatics

journal homepage: www.elsevier.com/locate/elstat

Controlled generation of single Trichel pulses and inherent EHD particle flow structures in a two-phase fluid (air and smoke particles)

Artur Berendt[a,*], Mateusz Tański[a], Jerzy Mizeraczyk[b]

[a] Institute of Fluid Flow Machinery, Polish Academy of Sciences, Fiszera 14, 80-231 Gdansk, Poland
[b] Department of Marine Electronics, Gdynia Maritime University, Morska 81-87, 81-225 Gdynia, Poland

A B S T R A C T

In this paper we presented results of the experiment on the use of controlled generation of a single Trichel pulse and a series of single Trichel pulses in the two-phase fluid (air + cigarette smoke particles). Also results of the monitoring the temporal and spatial evolution of the EHD smoke particles flow induced by these Trichel pulses in the needle-to-plate negative DC corona discharge arrangement in the closed discharge chamber are presented.

1. Introduction

The pulsed regime of a negative corona in the form of Trichel pulses has been experimentally and theoretically studied for over 80 years in gaseous single-phase fluids, mainly in air. The early (1938–1962) basic studies, carried out by Trichel [1], Loeb's group and others [2] concerned mostly the regular Trichel pulses of negative corona in air. Later the results of these early studies were analytically summarized and experimentally verified by Lama and Gallo [3]. The basic data and results of negative corona studies till 1980s were also collected in Refs. [4,5]. Afterwards hundreds of new papers on the various regimes of negative coronas (not only the Trichel-pulse regime) in air (i.e. in a single-phase fluid) have been published.

The negative coronas and inherent electrohydrodynamic (EHD) flows in gaseous two-phase gaseous fluids were studied mainly in terms of their practical aspects (breakdown voltage, back corona, dust particle collection efficiency, NOx production, etc.) important for the performance of electrostatic precipitators (ESPs). However, the investigations of the fundamentals of negative corona in two-phase gaseous fluids similar to that of the ESP flue gas (a mixture of an after-combustion gas and solid dust particles and microdroplets suspended in it) are scarce ([6–10]). Recently, due to an increasing interest in the electrical discharges in multi-matter environments, several new papers on the negative corona discharges in two-phase fluids have appeared [11–15].

This work was aimed at controlled generation of the single first Trichel pulse or series of single first Trichel pulses of the negative corona in a two-phase fluid, consisting of air and smoke particles suspended in it. Usually Trichel pulses are generated in the form of regular pulses, having a clearly distinguishing first pulse followed after a while by a Trichel pulse train [16–23]. The amplitude and duration of the first Trichel pulse, as well as its electric charge are substantially larger than those of the following pulses. The controlled generation of the single Trichel pulse (or series of such pulses) is expected to be helpful for the refined studies of the fundamental electrical and electrohydrodynamical processes in the negative corona discharge in two-phase (in general in multi-phase) gaseous fluids.

The idea of generating the single first Trichel pulse or series of single first Trichel pulses in the negative corona in the needle-to-plate electrode arrangement consists in generating the first Trichel pulse and supressing the next Trichel pulses (in the Trichel pulse train). This can be realized by applying an appropriately designed negative voltage pulse to the needle electrode. We propose to use a ramp voltage pulse with a fast rise time and much faster fall time. This enables precise controlling the ramp voltage pulse peak value in order to reach the peak voltage sufficient to generate the first Trichel pulse and to prevent the generation of the next Trichel pulse train pulses.

In this paper results of the use of the proposed for the generation of the single Trichel pulses (individually or in a series) and inherent EHD flow structures in a representative of the after-combustion two-phase fluid formed by air (at atmospheric pressure) seeded with cigarette smoke particles are presented. The experiment was performed in a discharge chamber with electrodes having the needle to plate electrode arrangement. The EHD smoke particle flow induced by the single Trichel pulse (or series of single Trichel pulses) was investigated using the time-resolved flow imaging system typical of the time-resolved PIV measurements [15,24,25].

2. Experimental set-up

The experimental apparatus for controlled generation of Trichel

* Corresponding author.
E-mail address: aberendt@imp.gda.pl (A. Berendt).

https://doi.org/10.1016/j.elstat.2018.01.007
Received 13 October 2017; Received in revised form 29 January 2018; Accepted 31 January 2018
Available online 06 February 2018
0304-3886/

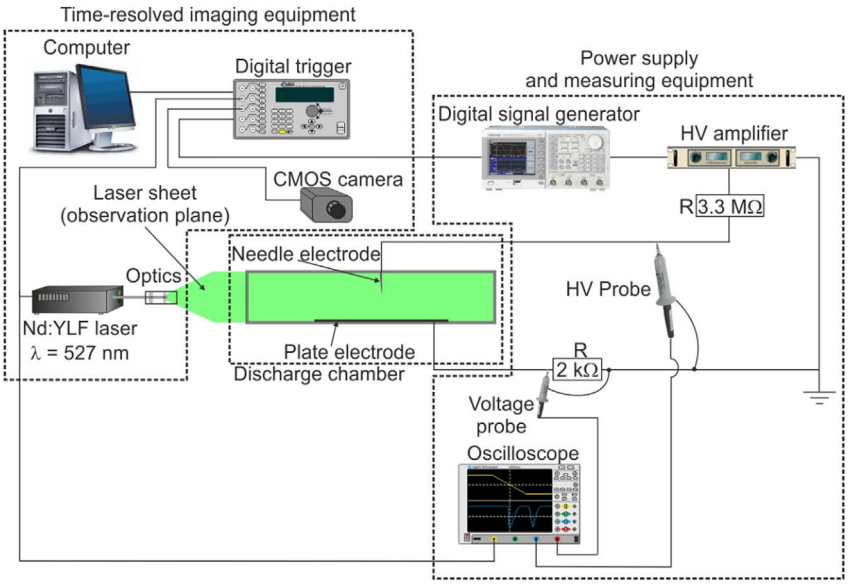

Fig. 1. Experimental set-up.

pulses consisted of a discharge chamber (a sealed acrylic box with a needle-to-plate electrode arrangement inside), a digital signal generator, a high voltage amplifier, two voltage probes, a digital oscilloscope and time-resolved EHD flow imaging equipment (Fig. 1).

2.1. Discharge chamber

The discharge chamber (acrylic box L:W:H = 600 mm: 120 mm: 50 mm) with the needle-to-plate electrode arrangement was filled with a two-phase fluid formed by ambient air seeded with cigarette smoke particles (the smoke particle concentration about 200 000 particles/cm^3 measured using an aerosol spectrometer Grimm 1.109, most of the cigarette smoke particles are submicron particles and their diameter ranges from 0.1 μm to 0.4 μm [26]).

The needle-to-plate electrode arrangement consisted of two electrodes: a needle and a plate. The both electrodes were made of stainless-steel. The needle electrode was a rod (1 mm in diameter), the end of which had a tapered profile. The tip of the needle electrode used for the generation of a single Trichel pulse had a radius of curvature of 75 μm, while the tip of the needle electrode used for the generation of a series of single Trichel pulses had a radius of curvature of 130 μm. The interelectrode gap between needle and plate electrode was 25 mm. The plate electrode was grounded.

2.2. Power supply and measuring equipment

The high voltage applied to the needle electrode was supplied by the high voltage amplifier (Trek, 40/15) which amplified voltage signal delivered by the digital signal generator (Tektronix, AFG 3052C). The negative high-voltage was applied to the needle electrode through a 3.3 MΩ resistor. The voltage between the needle electrode and the plate electrode was measured using a high-voltage probe (Tektronix, P6015A) and recorded by a digital oscilloscope (Keysight, DSO 9064A, bandwidth 600 MHz, sampling rate 10 GS/s). Using a voltage probe (Agilent, N2873A) the total current (consisting of the discharge and capacitive currents) waveform was measured as a voltage drop across a 2 kΩ resistor placed between the plate electrode and the ground. The voltage drop was recorded by the digital oscilloscope.

2.3. Time-resolved EHD particle flow imaging equipment

The time-resolved flow imaging system, sketched in Fig. 1, consisted of a twin Nd:YLF laser (Litron LDY304-PIV, pulse duration of 150 ns, pulse energy of 30 mJ with a repetition rate of 1000 Hz, wavelength λ = 527 nm), a laser sheet forming optics (cylindrical telescope), a high speed CMOS camera with lens (Speedsense M340, camera sensor size of 2560 pixels × 1600 pixels, acquisition rate of 800 Hz at full frame, acquisition rate can be increased at lower frame resolution), a digital trigger (digital delay/pulse generator BNC, Model 575) for triggering the laser pulses and the camera shutter, a computer with Dantec DynamicStudio software installed (typical of the time-resolved PIV measurements). The time-resolved EHD smoke particle flow imaging was carried out in the laser sheet plane (observation plane) passing along the discharge chamber in the needle-to-plate axis. To avoid reflections of the laser light on the needle electrode the laser sheet passed just below the needle electrode tip. More detailed description of our time-resolved imaging system and measurement procedure can be found in Ref. [14].

3. Results

3.1. Single Trichel pulse in two-phase fluid (air + smoke particles)

The first part of experiment 3.1 was aimed at the generation of a single Trichel pulse in the two-phase fluid (i.e. air seeded with smoke particles (particle concentration of 200 000 particles/cm^3)) and the monitoring of the induced EHD particle flow. The tip of the needle electrode used for this study had a radius of curvature of 75 μm.

First, we determined experimentally that the corona onset voltage was about – 3.9 kV. Second, we designed a voltage pulse waveform which was supposed to initiate a single Trichel pulse. The voltage pulse had the form of a ramp voltage pulse. The ramp voltage pulse was superimposed onto a DC negative component in order to maintain the negatively charged smoke particles moving towards the plate electrode after the disappearance of the Trichel pulse. We found that the negative ramp voltage pulse of an amplitude of about – 0.9 kV having a rise time of 1.5 ms and a fall time of 0.1 ms, superimposed onto the DC component of – 3 kV (Fig. 2) was capable of inducing a single Trichel pulse without any other following pulses (Fig. 3). Please notice that the current waveforms in this paper (Figs. 3, 4 and 7) are inverted with regard to the original oscilloscope display; as a result Trichel pulses, negative in the physical sense, are appear as “positive”. We believe that such presentation, also employed by other authors, is more readable.

As it can be seen from the total current and voltage waveforms

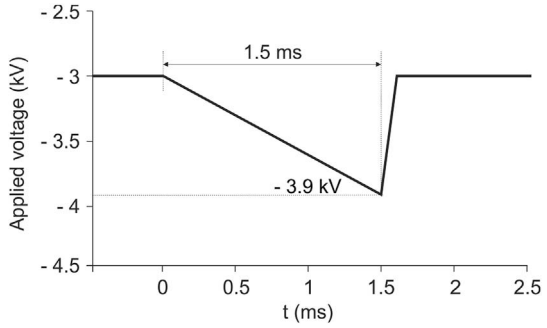

Fig. 2. The voltage pulse waveform for inducing a single Trichel pulse (a ramp voltage pulse superimposed onto a DC negative component).

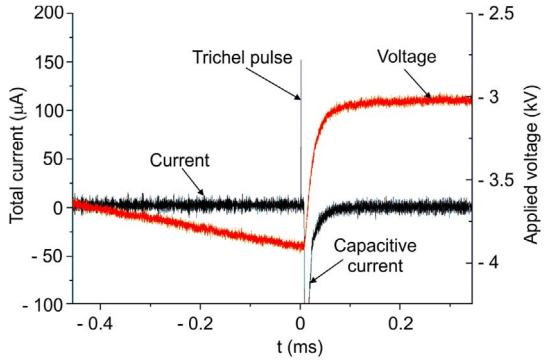

Fig. 3. Oscillograms showing the total current (the induced single Trichel pulse and the capacitive current) and voltage waveforms. The negative voltage pulse amplitude - 3.9 kV, the rise time - 1.5 ms, and the fall time - 0.1 ms.

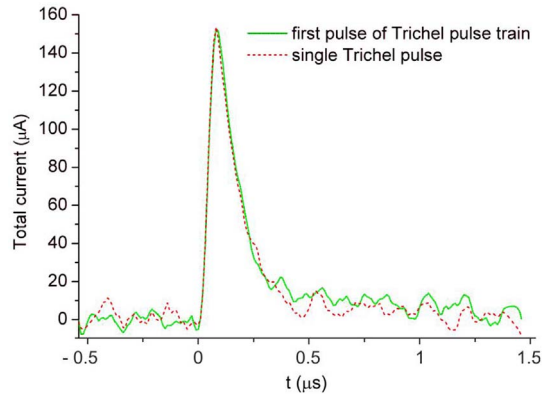

Fig. 4. Comparison of the single Trichel pulse generated in this experiment and the first pulse of the regular Trichel pulse train.

presented in Fig. 3 the applied voltage initiated a single discharge current pulse of an amplitude of about 150 μA. The rise time of the discharge current pulse was about 80 ns and its decay time was about 400 ns The single discharge current pulse injected an electric charge of approximately 40 pC into the system.

To ensure that the single discharge current pulse generated by the voltage pulse of a waveform shown in Figs. 2 and 3 is a Trichel pulse, we compared its shape with that of the first pulse of Trichel pulse train generated by us in the same experimental setup using a DC voltage of an amplitude of - 4.5 kV. As it can be seen in Fig. 4 the shapes of both compared pulses are almost the same, which allows us to concluded that the generated single discharge current pulse is the first Trichel pulse.

The second part of experiment 3.1 was devoted to monitoring the EHD smoke particle flow which inherently is induced by Trichel pulses in such a two-phase fluid [13–15]. For recording the time evolution of the EHD smoke particle flow the time-resolved EHD particle flow imaging equipment synchronised with the power supply equipment was used. The time evolution of the EHD smoke particle flow was recorded with a frame acquisition rate of the high speed CMOS camera set at 2000 frames per second (the frame resolution was reduced to 1280 pixel × 800 pixels). The total recording time was 500 ms. The time of the Trichel pulse onset in the recorded images was taken as a reference time $t = 0$. The images presenting the temporal and spatial evolution of the EHD smoke particle flow induced by the single Trichel pulse are shown in Fig. 5 (the corresponding total discharge current and voltage waveforms as in Fig. 3). Note that a higher intensity of a given area (i.e. a brighter area) in the image corresponds to a higher smoke particle concentration in this area. Dark or black areas in the image show a smaller concentration of particles or their absence in these areas.

In a separate experiment we found that almost immediately after the Trichel pulse initiation (i.e. after 20 μs– 30 μs) the EHD smoke particle flow was induced. At first, the EHD smoke particle flow manifested by the removal of electrically charged smoke particles from the very close vicinity of the needle electrode tip, forming a tiny dark area at the tip. Then this tiny dark area, emptied of the smoke particles, enlarged to form of a mushroom-like cap (Figs. 5a and 6b - t = 2 ms and t = 10 ms, respectively). As seen in Fig. 5a–f the smoke particles, pushed towards the plate electrode, formed a white layer on the surface of the dark mushroom cap. We call this white layer consisted of the smoke particles a mushroom front. With the time elapsing the mushroom-like smoke particle flow structure has grown and moved further towards the plate electrode.

When the mushroom-like smoke particle flow structure has continued its movement towards the plate electrode the smoke particles located above the needle electrode tip (not seen as not illuminated by the laser sheet in our experiment) began to inflow into the particle-free area under the needle electrode tip (compare Fig. 5c, t = 20 ms and Fig. 5d, t = 100 ms).

Fig. 5e (t = 200 ms) and 5f (t = 400 ms) show further development of the EHD smoke particle flow structure. As it can be seen the mushroom-like smoke particle flow structure has continued its growth and movement towards the plate. The volume of mushroom-like structure has increased during its movement towards the plate which means that the process of smoke particle removal by the mushroom front prevails over the reverse process of filling the particle-empty space left behind the mushroom front. This suggests a relative weakness of the forces which gas molecules exert on the smoke particles in the present fluid.

It can be found from the images presented in Fig 5a and f that initially the mushroom-like structure moved relatively fast and slowed down with the elapsing time. Such a behaviour is confirmed by a dependence of the distance of mushroom front from the needle tip on elapsing time (Fig. 6). As it can be seen from Fig. 6 the mushroom front propagation velocity was highest just after the Trichel pulse onset, i.e. in the close vicinity of the needle electrode tip. In the time period between t = 0 and t = 2 ms the maximum propagation velocity of mushroom front was about 0.6 m/s. Such a relatively high mushroom front propagation velocity in the close vicinity of the needle tip is justified by a relatively high electric field there (e.g. Refs. [27,28]; note the DC negative voltage remaining on the needle after the ramp pulse voltage decay). Then, in the time period between t = 2 ms and t = 50 ms the propagation velocity gradually decreased to about 0.23 m/s. In the time period between t = 50 ms and t = 500 ms the propagation velocity was almost constant and equal to about 0.02 m/s. In this time period the electric forces pushing the mushroom front towards the plate electrode are balanced by the hydrodynamic drag forces of the two-phase fluid compressed ahead of the mushroom front.

3.2. Series of the single Trichel pulses in two-phase fluid (air + smoke particles)

The first part of the experiment 3.2 was aimed at the controlled

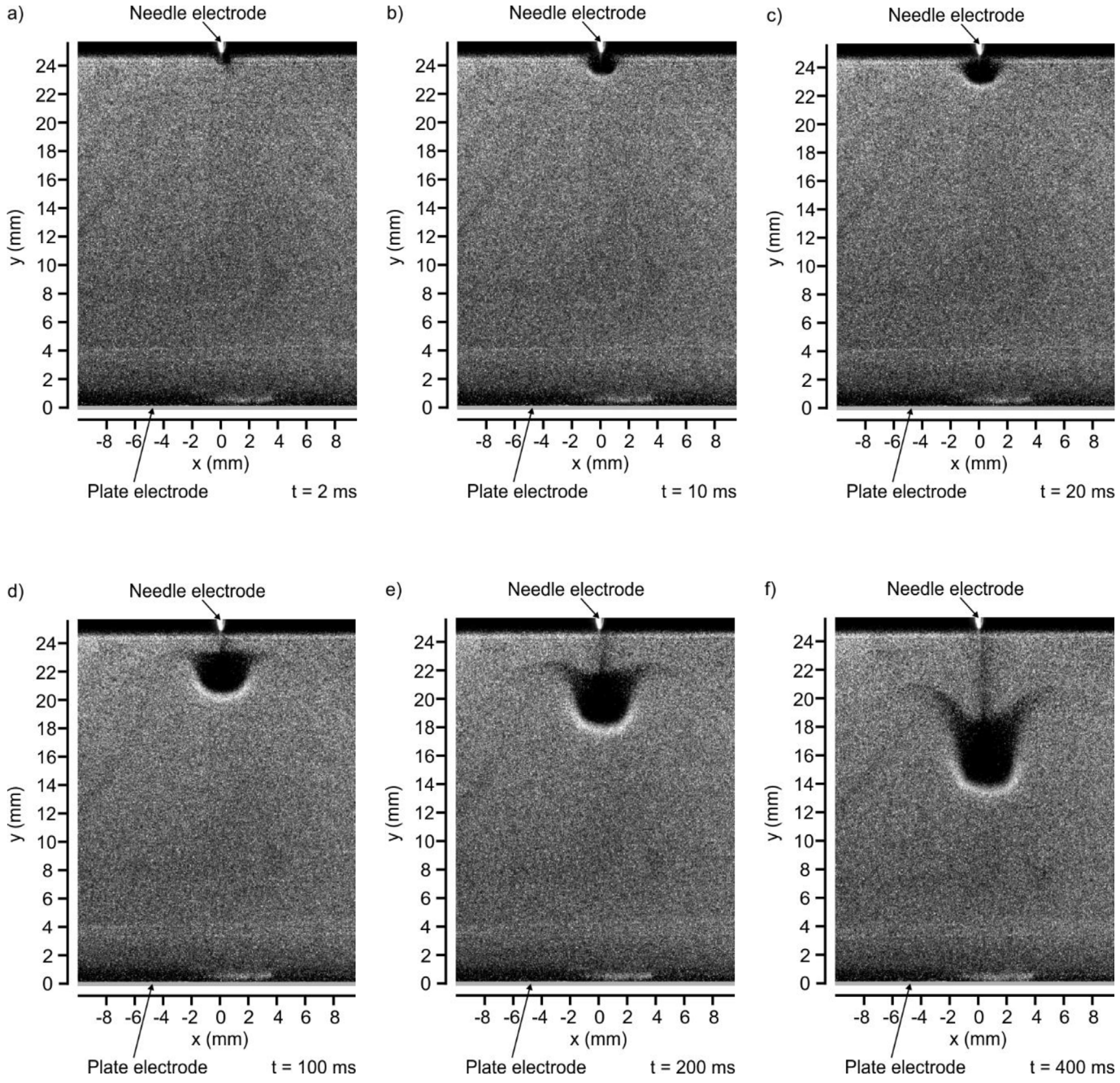

Fig. 5. Evolution of the EHD smoke particles flow induced by the single Trichel pulse generated by the voltage pulse shown in Figs. 2 and 3.

generation of a series of the single Trichel pulses in the two-phase fluid formed by air seeded with the smoke particles (particles concentration about 200 000 particles/cm^3) and monitoring the time evolution of the EHD smoke particle flow structures induced by the single Trichel pulse series. In this experiment (3.2) the tip of the needle electrode used had a radius of curvature of 130 μm. We designed the voltage waveform consisted of the ramp voltage pulses which were supposed to produce the series of the single Trichel pulses. Similarly as in the experiment 3.1 (Fig. 2) the ramp voltage pulses for producing the single Trichel pulse series were superimposed onto a DC negative component in order to maintain the negatively charged smoke particles flowing towards the plate electrode after the Trichel pulse disappearance. The lack of the DC component between the ramp voltage pulses may lead to the accumulation of the negative space electric charge in the vicinity of the needle tip and the discharge quenching.

We established that the parameters of the applied voltage waveform capable of producing a series of the single Trichel pulses have to be as follows: the period between the ramp voltage pules 50 ms (frequency 20 Hz), the amplitude of the ramp voltage pulses - 2.4 kV, the rise and fall times of ramp voltage pulses - about 40 ms and 0.2 ms, respectively, the DC component - 2.7 kV (which gives the maximum value of the total applied voltage - 5.1 kV). Note that the difference in the amplitude of the ramp voltage pulses and DC component voltage with respect to those of the experiment 3.1 is a result of the larger radius of needle tip curvature in the present experiment (130 μm versus 75 μm; the explanation can be found in Ref. [3]). The voltage waveform applied to the needle electrode and the resulting total current waveform are shown in Fig. 7. As shown in Fig. 7 each of the 5 ramp voltage pulses generated the single Trichel pulse. The amplitude of the Trichel pulses ranged from 350 μA to 420 μA. The electric charge injected into the system by the single Trichel pulse was about 85 pC. The higher Trichel pulse amplitude and injected electric charge than those of the

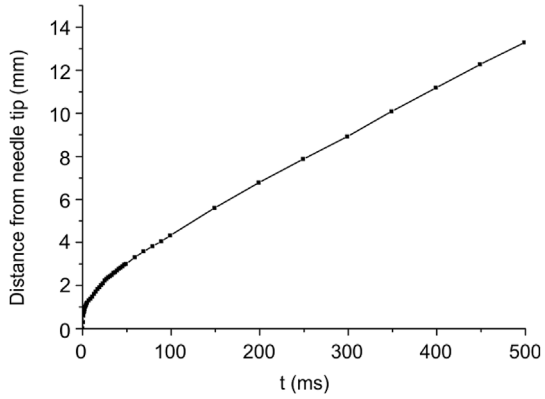

Fig. 6. Graph illustrating the propagation of the mushroom front induced by the single Trichel pulse in the two-phase fluid (air + smoke particles).

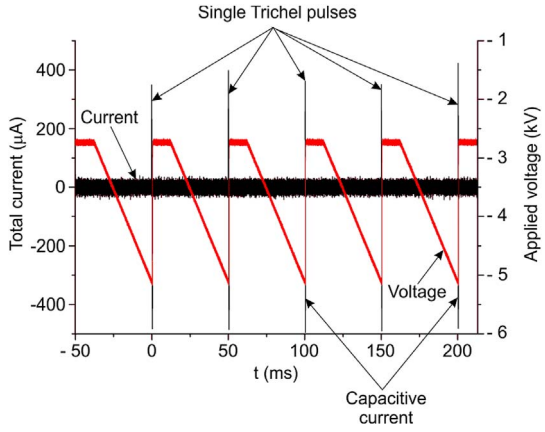

Fig. 7. The applied voltage waveform used for generation of a series of 5 single Trichel pulses in a row and the total current (the single Trichel pulses and capacitive current pulses) waveform are shown. The negative ramp voltage pulses (amplitude - 2.4 kV) was superimposed on the DC component (- 2.7 kV). The ramp voltage pulse rise and fall times are 40 ms and 0.2 ms, respectively. The frequency of the negative ramp voltage pulses and Trichel pulses is 20 Hz.

experiment 3.1 could be expected taking into account the larger radius of needle tip curvature in this experiment (3.2).

The second part of experiment 3.2 concerned the time evolution of the EHD smoke particle flow structures induced by the series of 5 single Trichel pulses monitored using the time-resolved EHD smoke particle flow imaging equipment. The parameters of recording the images of temporal and spatial evolution of EHD smoke particle flow structures were similar as those in the experiment 3.1 (the frame acquisition rate of the high speed CMOS camera - 500 frames per second, the total recording time - 500 ms) The time of the first Trichel pulse onset was taken in the following images as a reference time $t = 0$. The images showing the temporal and spatial evolution of the EHD smoke particle flow induced by the series of 5 single Trichel pulses (the corresponding total current and voltage waveforms as in Fig. 7) are shown in Fig. 8.

Fig. 8a shows the EHD smoke particle flow structure image captured 20 ms after the first Trichel pulse was generated. As seen after a time t = 20 ms the smoke particles has been removed from the vicinity of the needle tip and the bright layer of the smoke particles, forming the cap of the mushroom-like structure, headed towards the plate electrode.

The next image (Fig. 8b) was captured at a time t = 70 ms (i.e. 20 ms after the second single Trichel pulse generation). It shows that the first mushroom front has grown and moved away of the needle tip vicinity. The image also shows the second mushroom front formed by the second single Trichel near the tip of needle electrode.

In Fig. 8c (t = 120 ms, i.e. 20 ms after the third single Trichel pulse generation) further development of the EHD smoke particle flow is presented. It is seen that both the first and the second mushroom fronts have become larger when moving towards the plate electrode. Likely due to a lower hydrodynamic drag encountered by the second mushroom front, the second mushroom front has approached the first one and has begun to merged with the first mushroom front. In Fig. 8c also the generation of the third mushroom front, induced by the third single Trichel pulse is clearly seen. We established that the merging of the first and second mushroom fronts can be avoided if the time interval between the first and second single Trichel pulses is longer (in the experiment 3.2 the time interval between ramp voltage pulses is 50 ms).

The next image (Fig. 8d) presents the EHD particle flow structures at a time t = 170 ms (i.e. 20 ms after the fourth single Trichel pulse generation). In this moment the first and the second mushroom fronts have already merged together and have been moving together towards the plate electrode. The third mushroom front has been approaching the preceding particle flow structure to merge with it. Fig. 8d presents also the formation of the fourth mushroom front.

Fig. 8e (t = 220 ms, i.e. 20 ms after the fifth single Trichel generation) records the formation of the fifth mushroom front. The earlier generated mushroom fronts moved further towards the plate electrode.

The images in Fig. 8 clearly show that the series of 5 consecutive single Trichel pulses induced 5 mushroom fronts which travelled towards the plate electrode. A careful observation of the movement of consecutive mushroom fronts shows that each subsequent mushroom front has attained higher velocity than the preceding one (which causes that the distances between subsequent mushroom fronts decreases during their movement towards plate electrode). As mentioned above this due to setting an interelectrode flow channel by the first mushroom front, in which the following mushrooms front meet a lower hydrodynamic drag of the fluid and can reach higher velocities.

It is worth noting that the evolution of the EHD smoke particles flow induced by the series of 5 single Trichel pulses is similar to that induced by the 'naturally' generated Trichel pulses as described in Ref. [14].

4. Summary

In this paper we presented the results of experiment aimed at the controlled generation of the single Trichel pulses in the two-phase fluid (air + cigarette smoke particles) and monitoring the temporal and spatial evolution of the EHD smoke particles flow induced by these Trichel pulses in the needle-to-plate negative DC corona discharge arrangement in the closed discharge chamber.

In the first experiment (3.1) we generated the single Trichel pulse using the negative ramp voltage pulse superimposed on the DC component in the two-phase fluid (air + smoke particles). We found that the shape, amplitude, rise time and fall time of the generated single Trichel pulse were the same as those of the first Trichel pulse in the "regular" Trichel pulse train typical of the "standard" DC negative corona discharge.

The time-resolved EHD smoke particle flow images captured just after the single Trichel pulse generation showed that the smoke particles from the close vicinity of the needle electrode tip have fast been removed. The mushroom-like area free from the smoke particles was formed and moved towards the plate electrode. At the front of this area the plate electrode-pushed smoke particles formed a bright layer, called the mushroom front. The initial mushroom front propagation velocity was relatively fast (up to about 0.6 m/s). Then it gradually decreased with the elapsing time (0.02 m/s at 500 ms after the Trichel pulse initiation).

The second experiment (3.2) presented in this paper was aimed at the generation of the series of single Trichel pulses and monitoring the evolution of induced EHD smoke particle flow structures in the two-phase fluid (air + smoke particles). The series of 5 single Trichel pulses was successfully produced using the voltage consisted of 5 negative ramp voltage pulses superimposed on the DC component. The EHD smoke particle flow structure images showed that 5 mushroom-like

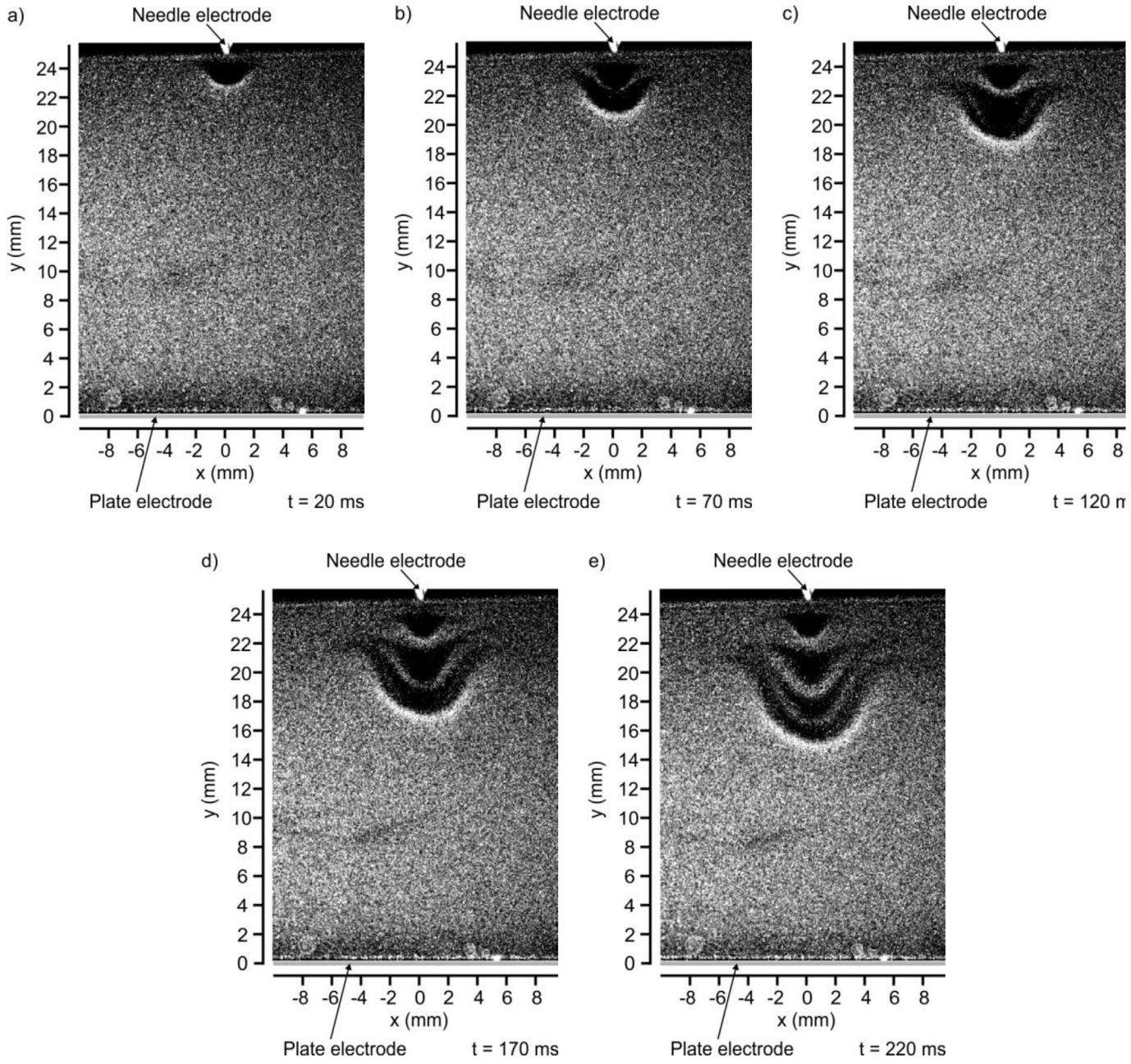

Fig. 8. Evolution of the EHD smoke particles flow structures induced by the series of 5 single Trichel pulses shown in Fig. 7.

smoke particle flow structures mushroom were induced by 5 single Trichel pulses. The evolution of these smoke particle flow structures resembled the evolution of the smoke particle flow structures induced by the "standard" negative DC corona (in the Trichel pulse regime) in the needle-to-plate electrode arrangement.

It is worth noticing that similar EHD particle flow structures in the air + smoke particles have been presented by us in Refs. [13–15]. However, the EHD particle structures shown there were generated by the trains consisted of uncontrolled number of Trichel pulses. Due to the inability of controlling the number of Trichel pulses there was impossible to determine how many Trichel pulses are needed to generate a single EHD particle flow mushroom-like structure. The present experiment showed that electric charge (about 40 10^{-12} C) carried by the single Trichel pulse is capable of generating a single EHD particle flow having the mushroom-like shape and transferring it away of the needle electrode.

The experimental results presented in this paper can be helpful for the validation of numerical models of the negative corona discharge in the two-phase fluid. It would contribute to a better understanding of the generation of negative corona discharge and processes induced by it (the particle charging and the EHD flow generation in the two-phase fluids are examples).

Acknowledgments

This work was supported by the National Science Centre (grant UMO-2013/09/B/ST8/02054).

References

[1] G.W. Tichel, Phys. Rev. 54 (1938) 1078–1084.
[2] L.B. Loeb, Electrical Coronas, Their Basic Physical Mechanisms, University of California Press, Berkely, CA, 1965.
[3] W.L. Lama, C.F. Gallo, J. Appl. Phys. 45 (1974) 103–113.
[4] R.S. Sigmond, J.M. Meek, J.D. Craggs (Eds.), Electrical Breakdown of Gases, Wiley,

New York, 1978.
[5] R.S. Sigmond, M. Goldman, E. Kunhardt (Ed.), Electrical Breakdown and Discharges in Gases Part B, Springer, US, 1981.
[6] J. Podlinski, A. Niewulis, J. Mizeraczyk, P. Atten, J. Electrost. 66 (2008) 246–253.
[7] J. Podlinski, A. Niewulis, J. Mizeraczyk, P. Atten, 6598, Proc. SPIE, 2007 65980Y.
[8] K. Adamiak, P. Atten, IEEE Trans. Dielectr. Electr. Insul. 16 (2009) 608–614.
[9] N. Farnoosh, K. Adamiak, G.S.P. Castle, IEEE Trans. Dielectr. Electr. Insul. 18 (2011) 1439–1452.
[10] Yu Akishev, G. Aponin, M. Grushin, V. Karalnik, A. Petryakov, N. Trushkin, IEEE Trans. Plasma Sci. 37 (2009) 1034–1044.
[11] B. He, Y. Li, D. Ma, R. Gu, M. Lin, Sci. China – Phys. Mech. Astron. 57 (2014) 1689–1695.
[12] B. He, T. Li, Y. Xiu, H. Zhao, Z. Peng, AIP Adv. 6 (2016) 035114.
[13] J. Mizeraczyk, A. Berendt, J. Podlinski, A. Niewulis, Int. J. Plasma Environ. Sci. Technol 10 (2016) 57–62.
[14] J. Mizeraczyk, A. Berendt, J. Podlinski, J. Phys. D Appl. Phys. 49 (2016) 205203.
[15] A. Berendt, J. Mizeraczyk, J. Electrostat. 84 (2016) 90–96.
[16] J.A. Scott, G.N. Haddad, J. Phys. D Appl. Phys. 19 (1968) 1507–1517.
[17] J.A. Cross, R. Morrow, G.N. Haddad, J. Phys. D Appl. Phys. 19 (1986) 1007–1017.
[18] Yu Akishev, M. Grushin, A. Napartovich, M. Pan'kin, N. Trushkin, Proc XII Int. Conf. On Gas Discharges and Their Applications, 1997, pp. 153–155 Greifswald, Germany.
[19] Yu Akishev, M. Grushin, I. Kochetov, A. Napartovich, N. Trushkin, Plasma Physics Report vol. 25, (1997), pp. 922–927.
[20] Yu Akishev, I.V. Kochetov, A. Loboiko, A.P. Napartovich, Plasma Physics Reports vol. 28, (2002), pp. 1049–1059.
[21] Yu Akishev, I. Kochetov, A. Napartovich, Proc. 8th Int. Symp. On High Pressure Low Temperature Plasma Chemistry, 2002, pp. 1–5. Tartu, Estonia.
[22] P. Sattari, G.S.P. Castle, K. Adamiak, Charlotte, U.S, Proc. ESA Annual Meeting on Electrostatics, 2010 Paper K4.
[23] P. Dordizadeh, K. Adamiak, G.S.P. Castle, J. Phys. D Appl. Phys. 48 (2015) 415203.
[24] A. Debien, N. Benard, L. David, E. Moreau, Appl. Phys. Lett. 100 (2012) 013901.
[25] M. Kotsonis, S. Ghaemi, J. Appl. Phys. 110 (2011) 113301.
[26] S.K. Sahu, M. Tiwari, R.C. Bhangare, G.G. Pandit, Aerosol Air Qual. Res. 13 (2013) 324–332.
[27] K. Adamiak, V. Atrazhev, P. Atten, IEEE Trans. Dielectr. Electr. Insul. 12 (2005) 1025–1034.
[28] M. Abdel-Salam, M. Nakano, A. Mizuno, J. Phys. D Appl. Phys. 40 (2007) 3363–3370.